Journal of Radioanalytical and Nuclear Chemistry (2023) 332:4191–4199
https://doi.org/10.1007/s10967-023-09081-2

Improved syntheses of $P2X_7$ ligands based on substituted benzyl amide of pyroglutamic acid motif labelled with iodine-123 or iodine-125

Anna Marešová[1] · Michal Jurášek[1] · Tomáš Zimmermann[1] · Pavel Drašar[1] · Miloš Petřík[2] · Petr Džubák[2] · Sture Lindegren[3] · Paul Cumming[4,5] · Robert Pichler[6,7] · Alexander Popkov[7,8,9]

Received: 23 May 2023 / Accepted: 25 July 2023 / Published online: 16 August 2023

Abstract

$P2X_7$ sites are emerging targets for molecular imaging research, notably in the context of neurodegeneration and inflammatory conditions. Therefore, we prepared a precursor for (radio)iodination of the $P2X_7$ ligand VPGIS191. We then developed a radioiodination method with ^{123}I for SPECT with a radiochemical yield of $71 \pm 13\%$ and ^{125}I for autoradiography with a radiochemical yield of $85 \pm 6\%$ Autoradiography of [^{125}I]VPGIS191 in mouse brain cryostat sections demonstrated approximately 36 nM binding affinity and B_{max} of approximately 400 pmol/gram tissue for $P2X_7$ binding sites. VPGIS191 (*cis*) had a two-fold lower affinity compared to its geometric *trans*-isomer TZ6019.

Graphical abstract

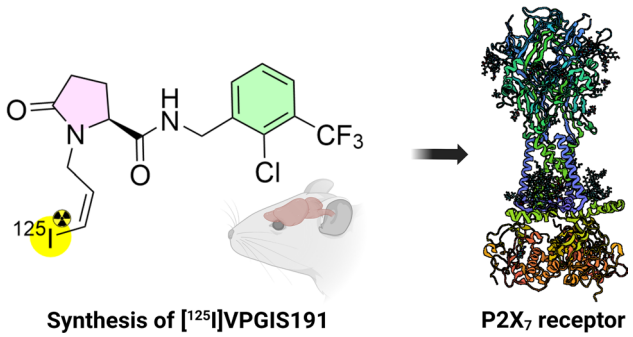

Keywords Radiopharmaceuticals · $P2X_7$ receptor · Autoradiography · Single photon emission tomography

✉ Michal Jurášek
michal.jurasek@vscht.cz

[1] Department of Chemistry of Natural Compounds, University of Chemistry and Technology Prague, Technická 5, 166 28 Prague 6, Czech Republic

[2] Institute of Molecular and Translational Medicine, Faculty of Medicine and Dentistry and Czech Advanced Technology and Research Institute, Palacky University Olomouc, Hněvotínská 5, 779 00 Olomouc, Czech Republic

[3] Department of Radiation Physics, Sahlgrenska University Hospital, Göteborg University, Blå stråket 5, 413 45 Göteborg, Sweden

[4] Department of Nuclear Medicine, University Hospital Bern, Freiburgstrasse 18, 3010 Bern, Switzerland

[5] Faculty of Health, School of Psychology and Counselling, Queensland University of Technology, Kevin Groove, Ring Rd, Queensland 4059, Australia

[6] Institut für Nuklearmedizin, Pyhrn-Eisenwurzen Klinikum Steyr, Sierninger Straße 170, 4400 Steyr, Austria

[7] Institute for Nuclear Medicine, Johannes Kepler University, Neuromed Campus, Wagner Jauregg Weg 15, 4020 Linz, Austria

[8] Samo Biomedical Centre, Na Klínku 1082, 530 06 Pardubice-Svítkov, Czech Republic

[9] Institute of Organic Chemistry, Johannes Kepler University, Altenberger Strasse 69, 4040 Linz, Austria

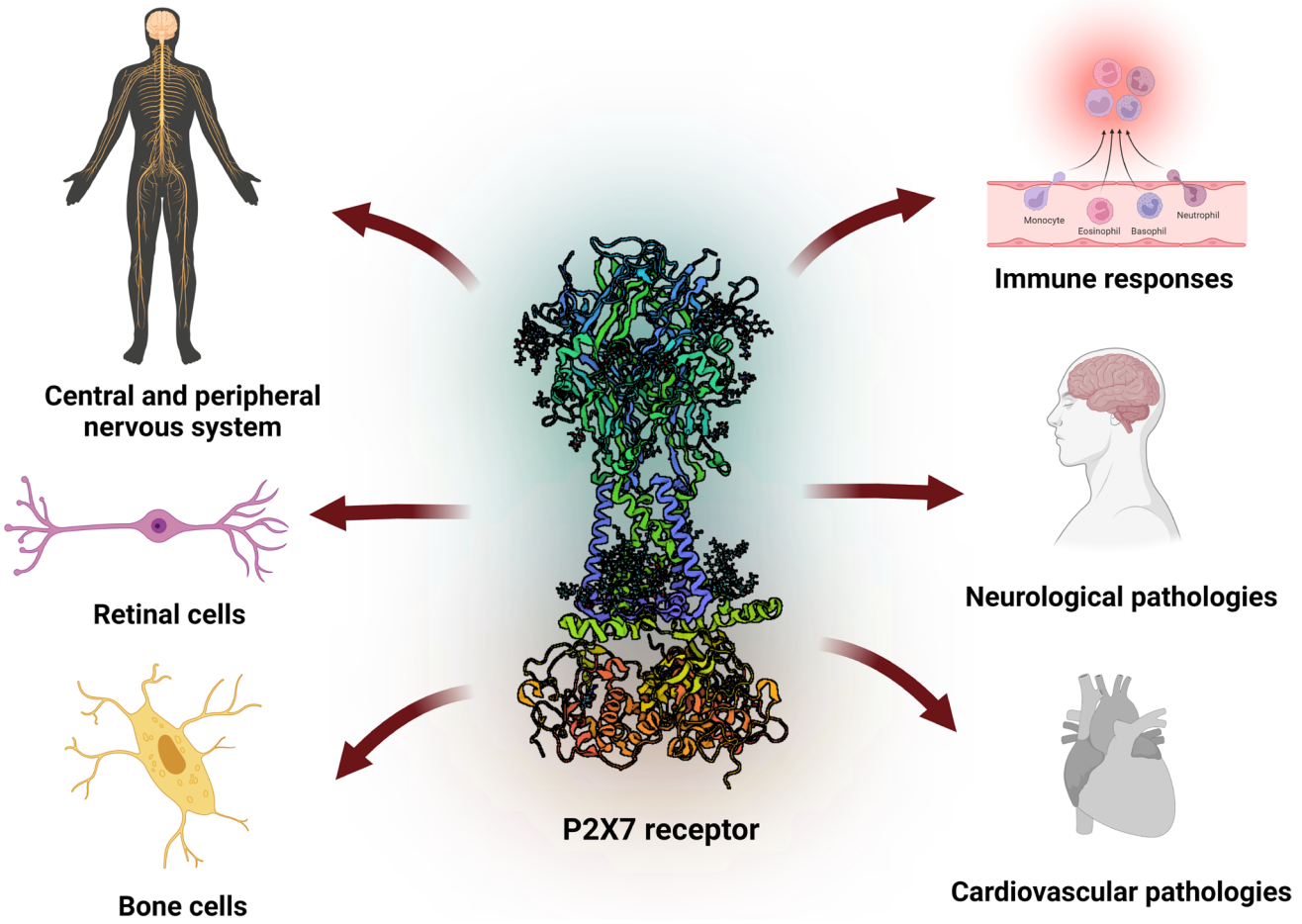

Fig. 1 Cartoon depicting the cellular locations of $P2X_7$ receptors and their predicted involvement in various pathologies with an inflammatory component. Created with BioRender.com

Introduction

$P2X_7$ (Fig. 1) is a transmembrane ligand-gated cation channel that is activated by extracellular adenosine triphosphate (ATP) and certain other adenosine nucleotides, thereby mediating cytokine release from cells of hematopoietic lineage such as microglia and macrophages in the brain, retina, and peripheral nervous system [1]. Activation of $P2X_7$ receptors mediates host immune responses participating in the regulation of apoptosis and inflammation [2] in a variety of pathologies including Alzheimer's and Parkinson's diseases [3], cardiovascular disorders [4], and cancers [5]. Due to their potential as markers or therapeutic targets in diverse disease conditions, $P2X_7$ receptors are an emerging topic for molecular imaging by positron emission tomography (PET) and single photon computer tomography (SPECT). However, clinical molecular imaging of $P2X_7$ receptors is in its infancy, in part due to the inadequate sensitivity of available radioligands [6].

The few $P2X_7$ ligands developed to date for molecular imaging have called for straightforward syntheses of precursors for simple [^{11}C]methylation or [^{18}F]fluorination for PET, and [^{123}I]iodination for SPECT. The main classes of these $P2X_7$ ligands are pyroglutamic acid-based (e.g. [^{11}C]GSK-1,482,160 [7], [^{123}I]TZ6019 [8]), triazole-based (e.g. [^{18}F]JNJ-64,413,739 [9], [^{3}H]JNJ-54,232,334 [10]) and adamantane-based compounds (e.g., [^{11}C]SMW139 [11]). The pyroglutamic acid-based radioligands identified thus far (Fig. 2) include [^{11}C]- or [^{18}F]GSK1482160 [7, 12], the [^{11}C]halo-GSK-1,482,160 analogs [9], [^{18}F]IUR-1601 and [^{18}F]IUR-1602 [13, 14], and [^{123}I]TZ6019 [8]. The characterization and preliminary results of their binding properties (K_i, IC_{50}, K_d, B_{max}) in HEK293 h$P2X_7$R (HEK) cells are shown in Table 1. Apart from [^{11}C]F-GSK1482160, [^{123}I]TZ6019 and [^{18}F]IUR-1602, the pyroglutamic acid-based ligands have high affinity for $P2X_7$. Notably, [^{11}C]GSK1482160 had 1.2 ± 0.1 nM affinity (K_d) [15] versus 19.3 ± 2.8 nM for [^{123}I]TZ6019 [8]. These lead compounds for PET and SPECT

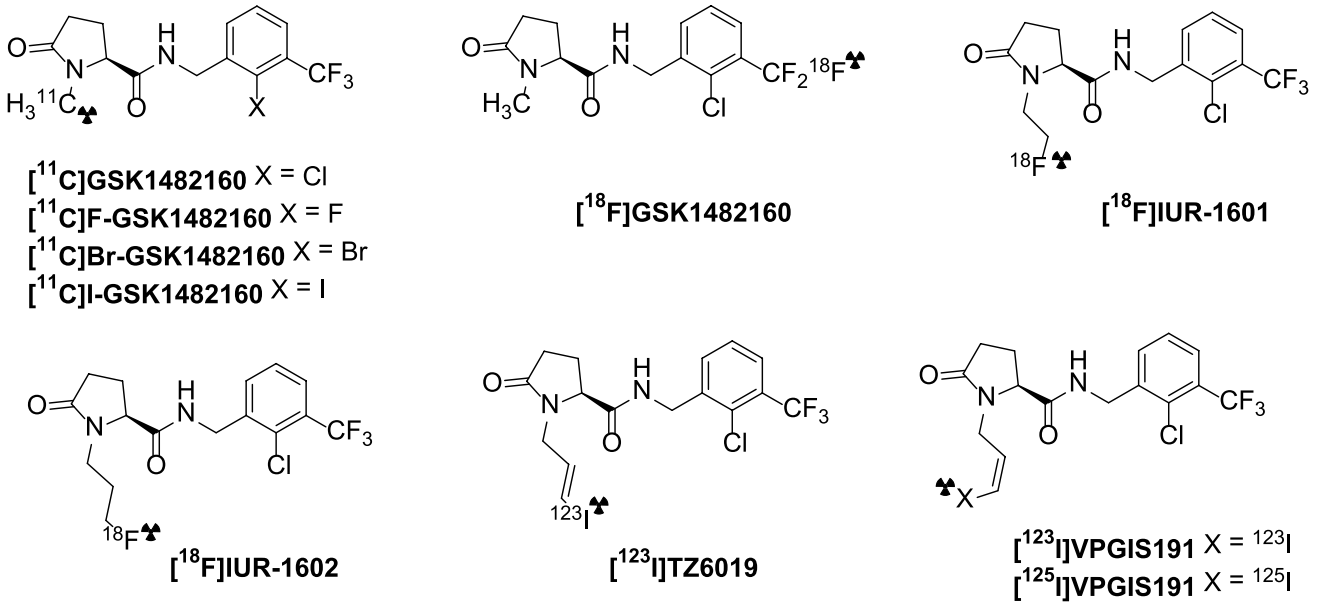

Fig. 2 Pyroglutamic acid-based $P2X_7$ ligands

Table 1 Preliminary biological evaluation of $P2X_7$ receptor radioligands with respect to inhibitory constant (K_i), half-maximal inhibitory concentration (IC_{50}), dissociation constant (K_d), and maximum specific binding (B_{max}) in HEK cells

Radioligand	K_i [nM]	IC_{50} [nM]	K_d [nM]	B_{max} [fmol/mg protein]
[^{11}C]GSK1482160	5.1 ± 0.9[a] [13] 2.63 ± 0.6 [16] 3.1 ± 0.3 [9]	7.17 [13] 3 [6] 4.3 ± 0.86 [8]	5.1 ± 1.0 [16] 1.2 ± 0.1 [15]	3 030 ± 100 [15]
[^{11}C]F-GSK1482160	54.2 ± 6.2 [9]	152.6 ± 17.5 [9]	ND	ND
[^{11}C]Br-GSK1482160	2.5 ± 0.7 [9]	7.1 ± 1.9 [9]	ND	ND
[^{11}C]I-GSK1482160	1.9 ± 0.6 [9]	5.3 ± 1.5 [9]	ND	ND
[^{18}F]GSK1482160	ND	ND	ND	ND
[^{18}F]IUR-1601	4.3 ± 0.9[a] [13]	7.86 [13]	ND	ND
[^{18}F]IUR-1602	23.6 ± 1.0[a] [14]	ND	ND	ND
[^{123}I]TZ6019	6.3 ± 0.9 [8]	9.5–12.9[b] [6]	19.3 ± 2.8 [8]	262 ± 10 [8]

[a] radioligand competitive binding assay using [^{11}C]GSK1482160 in HEK cells

[b] in different HEK cell assays: [^{123}I]TZ6019, fluorescence, [^{3}H]A-804,598 binding assay

imaging present unexplored opportunities for structural modification alternative radiosynthetic routes.

The only published report of a SPECT ligand for $P2X_7$ receptors indicated moderate affinity and specific binding of [^{123}I]TZ6019 in HEK cells [8]. However, the [^{123}I]TZ6019 was prepared from commercially unavailable (*E*)-(3-bromoprop-1-en-1-yl)-tributylstannane, which has likely impeded the broader use of the radioligand. Our compilation of literature data led us to note that *E*-3-iodoallyl-derived radioligands often demonstrate slightly higher affinity for their various receptor targets as compared to *Z*-3-iodoallyl-derived radioligands [17–20]. Therefore, we determined to prepare the [^{123}I]TZ6019 geometric *Z*-isomer from commercially available (*Z*)-(3-bromoprop-1-en-1-yl)-tributylstannane, and evaluate its binding to $P2X_7$ receptors in rodent brain sections. In this study, we describe the syntheses of a VPGIS191 precursor and the VPGIS191 chromatographic standard, and procedures for precursor iodination with ^{123}I for SPECT and ^{125}I for autoradiography. Finally, we made a preliminary evaluation of [^{125}I]VPGIS191 binding to $P2X_7$ receptors in mouse brain cryostat sections, comparing our results with previously reported K_D/B_{max} values for [^{123}I]TZ6019 in HEK cells.

Experimental

General methods

For thin-layer chromatography (TLC), we used aluminium silica gel sheets with detection in UV light (TLC silica

gel 60 F254, Merck). For TLC visualization, we applied a dilute solution of H_2SO_4 in MeOH and heated the plates. For column chromatography, we used 30–60 µm silica gel (ICN Biomedicals, Costa Mesa, USA). NMR spectra were recorded using Agilent-MR DDR2 (Varian, Palo Alto, USA). HRMS were measured using an LTQ ORBITRAP VELOS with $HESI^+$/$HESI^-$ ionization (Thermo Scientific, Waltham, MA, USA). A quadrupole LC/MS-ESI with an Infinity III LC system (Agilent Technologies, Santa Clara, USA) served for LR-MS and HPLC-MS analyses (10 µm C_{18} column: 100 mm; UV detection). For the characterization of radioactive products, we undertook HPLC analyses (C_{18} columns, UV, and RAD detections). Purification procedures employed SPE columns (Bond Elut Plexa, Agilent Technologies, Santa Clara, USA, and Strata, Phenomenex, Torrance, USA). Materials for quantitative autoradiography included brains of female Balb/c mice (Palacky University, Olomouc, Czech Republic), Tissue-Tek gel (Sakura, Torrance, USA), Superfrost plus microscope slides (Fisher Scientific, Hampton, USA), a microtome cryostat (Leica Biosystems, IL, USA), phosphor storage screens (BAS), and a Cyclone Plus Phosphor Imager (PerkinElmer, Waltham, USA).

Materials

Bachem (Bubendorf, Switzerland): L-pyroglutamic acid (> 99.0%); Lach-Ner (Neratovice, Czech Republic): dichloromethane (99%); Sigma-Aldrich (Missouri, USA): acetic acid (99.7%), benzylamine (99%), 1-(3-dimethylaminopropyl)-3-ethylcarbodiimide hydrochloride (≥ 98%), dimethylformamide (≥ 99.8%), chloroform (≥ 99%), hexane (95%), hydrochloride acid (37%) 1-hydroxybenzotriazole hydrate (≥ 97%), lithium bis(trimethylsillyl)amide (1 M solution in THF), N-iodosuccinimide (95%), methyl trifluoromethanesulfonate (≥ 98%), sodium chloride (≥ 99.0%), (+)-sodium L-ascorbate (≥ 98%), sodium sulphite (≥ 98%), tetrabromomethane (99%), tetrabutylammonium hydroxide (≥ 99.0%), tetrahydrofuran (≥ 99.0%), trifluoroacetic acid (≥ 99.0%), triphenylphosphine (99%); Synthonix (Wake Forest, USA): (*Z*)-3-(tributylstannyl)prop-2-en-l-ol (> 99%); VWR (Radnor, USA): 2-chlor-3-(trifluormethyl)benzylamine (≥ 97%). The solvents for column chromatography and reactions for the synthesis of **VPGIS191** were purchased from PENTA (Prague, Czech Republic) and were used as delivered (all of p.a. quality). For radio-iodinations, sodium iodide I^{123} (37 MBq/mL) with sodium chloride, sodium hydrogen carbonate and water for injection were from THP Medical Products Vetriebs GmbH (Wien, Austria). Sodium iodide I^{125} (3550 MBq/mL) solution in sodium hydroxide was purchased from Izotop (Budapest, Hungary).

Syntheses of 1, and a precursor for VPGIS191

(*S*)-*N*-(2-Chloro-3-(trifluoromethyl)benzyl)-5-oxopyrrolidin-2-carboxamide (**1**): To a solution of 2-chloro-3-(trifluoromethyl)phenyl)methanamine (650 mg, 3.1 mmol) in 30 mL of dry CH_2Cl_2 L-pyroglutamic acid (426 mg, 3.3 mmol), *N*-hydroxybenzotriazole (HOBt, 502 mg, 3.7 mmol) and ethyl(dimethylaminopropyl)carbodiimide (EDCI, 713 mg, 3.7 mmol) were added, respectively. The mixture was put aside at room temperature for 14 h, whereupon solvents were removed under reduced pressure and the residue was purified by column chromatography in $CHCl_3$-MeOH (20:1–10:1, *v*/*v*) to give **1** (649 mg, 2 mmol, 61%) as a colorless solid. After lyophilization, the product was stored at 4 °C as a white foam. R_F = 0.25 in CH_2Cl_2-MeOH 20:1 (*v*/*v*). ^{1}H NMR (400 MHz, acetone-d_6) δ ppm: 2.07–2.33 (m, 3 H), 2.40–2.52 (m, 1 H), 4.25 (dd, *J* = 9.0, 3.9 Hz, 1 H), 4.53–4.65 (m, 2 H), 7.29 (br s, 1 H), 7.47–7.54 (m, 1 H), 7.72 (t, *J* = 6.7 Hz, 2 H), 8.10 (br s, 1 H). ^{13}C NMR (101 MHz, acetone-d_6) δ ppm: 27.01 (*C*H_2, pyrr), 41.82 (*C*H_2, pyrr), 57.83 (NH-*C*H_2), 124.50 (q, *J* = 272.4 Hz, *C*F_3), 127.65 (q, *J* = 5.6 Hz, Ar*C*H), 128.45, 129.21 (q, *J* = 30.5 Hz, Ar*C*H), 131.65 (d, *J* = 1.5 Hz, Ar*C*H), 134.10 (Ar*C*H), 134.12 (Ar*C*H), 140.53 (Ar*C*H), 174.21 (-NH*C*=O), 179.01 (*C*=O, pyrr). MS-ESI: for $C_{13}H_{12}ClF_3N_2O_2$ calcd. 320.05 Da, found 338.7 $[M+NH_4]^+$.

(*S*,*Z*)-*N*-(2-Chloro-3-(trifluoromethyl)benzyl)-5-oxo-1-(3-(tributylstannyl)allyl)pyrrolidine-2-carboxamide (**2**): Step 1. To a solution of (*Z*)-3-(tributylstannyl)prop-2-en-l-ol (1 g, 2.9 mmol) in 40 mL of THF triphenylphosphine (982 mg, 3.7 mmol) and CBr_4 (1.23 g, 3.7 mmol) were added. The mixture was stirred at 0 °C (on ice) for 3 h, and then at room temperature for 14 h. The solvents were removed under reduced pressure and the residue was purified by column chromatography with hexane to give (*Z*)-(3-bromprop-l-en-l-yl)tributylstannane [21] (800 mg, 1.95 mmol, 68%) as a colorless liquid. The product thus obtained was used directly in the next reaction. ^{1}H NMR (400 MHz, $CDCl_3$) δ ppm: 0.80–0.87 (m, 15 H), 1.18–1.30 (m, 6 H), 1.38–1.46 (m, 6 H), 3.89 (dd, *J* = 6.7, 0.9 Hz, 2 H), 6.05 (dt, *J* = 18.5, 6.6 Hz, 1 H), 6.22 (d, *J* = 18.7 Hz, 1 H). ^{13}C NMR (101 MHz, $CDCl_3$) δ ppm: 9.6, 13.7, 27.2, 29.0, 35.8, 135.1, 143.0.

Step 2. To a solution of **1** (300 mg, 0.93 mmol) in 5 mL of DMF, stirred under an atmosphere of argon at 0 °C (on ice), 2 mL of lithium bis(trimethylsilyl)amide solution in THF (1 M) was added. Thereafter, (*Z*)-(3-bromprop-l-en-lyl) tributylstannane (800 mg, 1.95 mmol) was added dropwise. The mixture was stirred at 0 °C (on ice) for 10 min, and then at room temperature for 3 h, whereupon the reaction was stopped by adding 25 mL of aqueous HCl (1 M). The resultant mixture was extracted with EtOAc (3 × 50 mL). The combined organic layer was washed with a saturated

solution of NaCl (2 × 50 mL) and dried over Na_2SO_4. The solvent was evaporated under reduced pressure and the residue was purified by column chromatography (hexane-EtOAc 4:1–1:2, *v*/*v*) to give **2** (268 mg, 3.7 mmol) as a pale-yellow viscous substance. $R_F = 0.3$ in hexane-EtOAc 1:1. The product was visualized on TLC by gaseous iodine (brown spot). The product **2** was injected onto an analytical HPLC (YMC-Triart C_{18} column, 150 × 4.6 mm, 5 µm; gradient 40/60–90/10, *v*/*v* AcCN/0.1% TFA, 1 mL/min, t_R = 28 min). ^{1}H NMR (400 MHz, $CDCl_3$) δ ppm: 0.75–0.98 (m, 15 H, overlap 3×CH_2 a 3×CH_3), 1.18–1.37 (m, 6 H, 3×CH_2), 1.37–1.51 (m, 6 H, 3×CH_2), 1.96–2.10 (m, 1 H, C*H*), 2.16–2.53 (m, 3 H, overlap, 3×C*H*, 1×CH_2), 3.51 (br dd, *J* = 14.9, 7.4 Hz, 1 H, C*H*), 4.07 (br dd, *J* = 9.2, 2.5 Hz, 1 H, C*H*), 4.21 (br dd, *J* = 14.9, 5.5 Hz, 1 H, C*H*), 4.58 (d, *J* = 5.9 Hz, 1 H, C*H*), 6.04 (br d, *J* = 12.5 Hz, 1 H, C*H*), 6.28 (ddd, *J* = 12.8, 7.3, 5.7 Hz, 1 H, C*H*), 7.07 (br t, *J* = 5.7 Hz, N*H*), 7.29–7.36 (m, 1 H, C*H*), 7.56 (br d, *J* = 7.4 Hz, 1 H, C*H*), 7.63 (br d, *J* = 7.8 Hz, 1 H, C*H*). ^{13}C NMR (101 MHz, $CDCl_3$) δ ppm: 10.23 (d, J_{CSn} = 343.3 Hz, 3×*C*H_2), 13.66 (3×*C*H_3), 24.21 (*C*H_2, pyrr), 27.23 (d, $J_{C\text{-}Sn}$ = 58 Hz, 3×*C*H_2), 28.08 (d, $J_{C\text{-}Sn}$ = 21.4 Hz, 3×*C*H_2), 29.52 (1×*C*H_2, pyrr), 41.48 (NH-*C*H_2), 47.24 (d, $J_{C\text{-}Sn}$ = 38.9 Hz, N-*C*H_2), 60.90 (*C*H, pyrr), 122.75 (q, *J* = 273.6 Hz, *C*F_3), 126.94 (q, $J_{C\text{-}F}$ = 5.9 Hz, Ar*C*H), 129.06 (q, $J_{C\text{-}F}$ = 31.3 Hz, Ar*C*H), 131.60 (d, $J_{C\text{-}F}$ = 1.5 Hz, Ar*C*H), 133.47 (Ar*C*H), 134.60 (d, $J_{C\text{-}Sn}$ = 339.52 Hz, = *C*H) 134.61 (Ar*C*H), 137.78 (Ar*C*H), 141.61 (= *C*H) 171.64 (-NH*C* = O), 175.51 (*C* = O, pyrr). MS-ESI: for $C_{28}H_{42}ClF_3N_2O_2Sn$ calcd. 650.2 Da, found *m*/*z* 651.2 $[M+H]^+$.

(*S*,*Z*)-*N*-(2-Chloro-3-(trifluoromethyl) benzyl)-1-(3-iodoallyl)-5-oxopyrrolidine-2-carboxamide (VPGIS191):

Method I. To a solution of **2** (6.5 µg, 10 nmol) in 20 µL 1% acetic acid in MeOH was added 4 µL *N*-iodosuccinimide (10 mg/mL 1% acetic acid in MeOH). The mixture was stirred at RT for 15 min, whereupon the reaction was stopped with sodium thiosulfate (5 mg, 1.6 nmol). Subsequently, the mixture was diluted with 1 mL of distilled water and passed through a preconditioned SPE cartridge (2 mL, 20% EtOH), and eluted with 2 mL of 80% EtOH. The product **3** was injected onto an analytical HPLC (YMC-Triart C_{18} column, 150 × 4.6 mm, 5 µm; gradient 40/60–90/10, *v*/*v* AcCN/0.1% TFA, 1 mL/min, t_R = 12 min).

Method II. To a solution of **2** (32.5 mg, 0.05 mmol) in 3 mL of $CHCl_3$ was added 0.5 mL solution of iodine in $CHCl_3$ (0.1 M) dropwise. The mixture was stirred at RT for 20 h, and then diluted with 4 mL of $CHCl_3$, and washed with saturated solution of first $Na_2S_2O_3$ (6 × 15 mL), and then with a saturated solution of NaCl (15 mL). The combined organic layer was dried over Na_2SO_4. The solvents were removed under reduced pressure and the residue was purified by column chromatography $CHCl_3$-MeOH (20:1–10:1, *v*/*v*) to give **VPGIS191** (12.7 mg, 52%) as a brown solid. The product was injected onto an analytical HPLC (YMC-Triart C_{18} column, 150 × 4.6 mm, 5 µm; gradient 40/60–90/10, *v*/*v* AcCN/0.1% TFA, 1 mL/min, t_R = 12 min). ^{1}H NMR (400 MHz, $CDCl_3$) δ ppm: 2.02–2.12 (m, 1 H), 2.27–2.41 (m, 2 H), 2.50–2.61 (m, 1 H), 3.75 (br dd, *J* = 15.5, 7.6 Hz, 1 H), 4.00 (br dd, *J* = 8.6, 2.7 Hz, 1 H), 4.25 (br dd, *J* = 15.3, 5.1 Hz, 1 H), 4.63 (d, *J* = 5.9 Hz, 2 H), 6.11 (br q, *J* = 7.4 Hz, 1 H), 6.38 (br d, *J* = 7.8 Hz, 1 H), 7.37 (t, *J* = 7.4 Hz, 1 H), 7.66 (br dd, *J* = 7.6, 2.5 Hz, 2 H).^{13}C NMR (101 MHz, $CDCl_3$) δ ppm: 23.76, 29.40, 41.83, 46.17, 61.02, 86.62, 121.36, 124.08, 127.01, 127.31 (q, $J_{C\text{-}F}$ = 5.3 Hz), 129.34, 134.34, 134.89, 137.44, 171.31, 175.76. MS-ESI: for $C_{16}H_{15}ClF_3IN_2O_2$ calcd. 486.7 Da, found *m*/*z* 504.7 $[M+NH_4]^+$.

Manual syntheses of iodine-123 or iodine-125 labelled VPGIS191

(*S*,*Z*)-*N*-(2-Chloro-3-(trifluoromethyl)benzyl)-1-(3-[^{125}I] iodoallyl)-5-oxopyrrolidine-2-carboxamide (**1** [^{125}I] VPGIS191): To a solution of **2** (6.5Sch µg, 10 nmol) in 20 µL 1% acetic acid in MeOH were added 23.5 MBq [^{125}I] NaI and chloramine-T (2 µL, 10 mg/mL). The mixture was stirred at RT for 10 min, and the reaction was stopped with sodium ascorbate (5 µL, 50 mg/mL). Subsequently, the mixture was diluted with 2 mL of distilled water and 1 mL of 1% acetic acid in MeOH and passed through a preconditioned SPE cartridge (2 mL, 20% EtOH, Bond Elut Plexa, Agilent) and eluted with 1.5 mL of 60% EtOH. The product [^{125}I]VPGIS191 was isolated 20 MBq with 85% radiochemical yield (RCY, Tab. S1). The product was injected onto an analytical HPLC (YMC-Triart C_{18} column, 150 × 4.6 mm, 5 µm; gradient 40/60–90/10, *v*/*v* AcCN/0.1% TFA, 1 mL/min, t_R = 12 min).(*S*,*Z*)-*N*-(2-Chloro-3-(trifluoromethyl)benzyl)-1-(3-[^{123}I]iodoallyl)-5-oxopyrrolidine-2-carboxamide ([^{123}I]VPGIS191) (**[^{123}I] VPGIS191**): To a solution of **2** (6.5 µg, 10 nmol) in 20 µL 1% acetic acid in MeOH were added 12.3 MBq [^{123}I] NaI and chloramineT (2 µL, 10 mg/mL). The mixture was stirred at RT for 20 min, and the reaction was then stopped with sodium ascorbate (5 µL, 50 mg/mL). Subsequently, the mixture was diluted with 2 mL of distilled water and 1 mL of 1% acetic acid in MeOH, passed through a preconditioned SPE cartridge (2 mL, 20% EtOH, Strata, Phenomenex), and then eluted with 1.5 mL of 70% EtOH. The product [^{123}I]VPGIS191 was isolated at 10.4 MBq, corresponding to 85% RCY **(Tab. S2).**

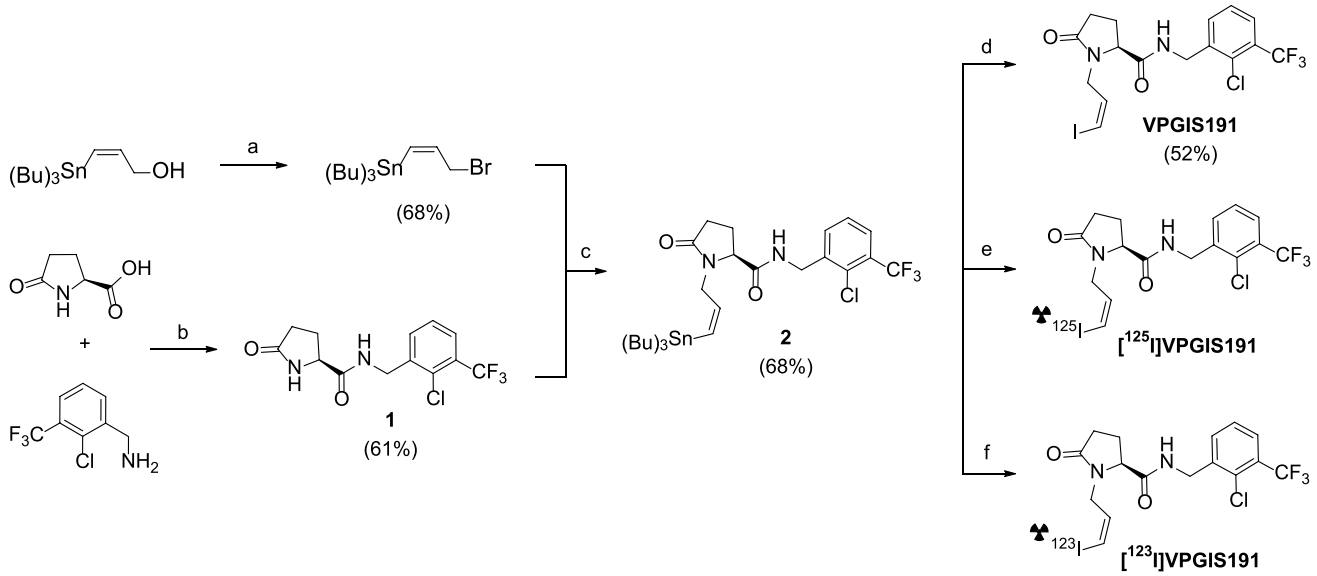

Scheme 1 Synthesis of the $P2X_7$ receptor ligand **VPGIS191** and its radio-iodination. *Reagents and conditions*: (a) PPh_3, CBr_4, THF, 0 °C → 20 °C, 17 h; (b) EDCI, HOBt, CH_2Cl_2, RT, 12 h; (c) (*Z*)-(3-bromoprop-1-en-1-yl)-tributylstannane, LHMDS in THF, DMF, 0 °C → RT, 3 h; (d) Method (I) NaI, chloramine-T, MeOH, AcOH, sodium ascorbate, RT, 5 min; Method (II) I_2, $CHCl_3$, RT, 20 h; e) $Na^{125}I$, chloramine-T, MeOH, AcOH, sodium ascorbate, RT, 5 min; f) $Na^{123}I$, chloramine-T, MeOH, AcOH, sodium ascorbate, RT, 5–20 min

In vitro autoradiography

We followed an autoradiographic procedure much as described by Kuhar et al. [22]. Saline-perfused mouse brains were frozen by immersion to isopentane at − 40 °C, and stored at − 80 °C until use. A cerebral hemisphere was mounted in the sagittal orientation in a cryostat for cutting at − 20 °C into 20 µm-thick sections, which were thaw-mounted onto Superfrost glass slides. After air-drying and storage overnight at − 80 °C, the slides were preincubated in buffer (50 mM buffer: Tris-HCl, pH 7.4, 1 mM EDTA, 0.1% BSA) for 15 min. After removal of the excess buffer, the slides were incubated with the same buffer (1 mL) modified by addition of radiotracer [^{125}I]VPGIS191 (A_m = 4.6 MBq/nmol) at final concentrations of 2, 10, 50 and 100 nM. Nonspecific binding was evaluated in consecutive brain sections by the addition of GSK1482160 to a final concentration of 10 µM. After one-hour incubation, the sections were washed by immersion in ice cold buffer (3 × 1 min) and finally dipped in distilled water (30 s, 5 °C) to remove buffer salts, followed by rapid drying under an air stream. The dried slides were then exposed to a phosphor storage screen for 1 − 6 min together with slides bearing dried drops of buffer of known concentrations of The imaging screens were read using a Cyclone phosphor imager (Perkin-Elmer, USA), and the brain binding results (total, non-specific, and specific) converted into units of pmol/gram tissue (wet weight).

Data analysis

Data from autoradiography experiments were analyzed using Microsoft Excel (Microsoft, Redmond, WA, USA). The saturation binding parameters (B_{max} and K_d) were determined using linear regression of the Scatchard plot.

Results and discussion

Chemical synthesis and radiochemistry

The preparation of amide **1** was carried out according to the procedure previously described using the reagent 1-ethyl-3-(3-dimethylaminopropyl)carbodiimide (EDCI) with the addition of *N*-hydroxybenzotriazole (HOBt) as a catalyst [7]. The reaction and isolation of the product were unproblematic, although the 61% yield fell short of the 76% reported in the literature [7]. We produced (*Z*)-(3-bromoprop-1-en-1-yl)tributylstannate from the commercially available (*Z*)-3-(tributylstannyl)prop-2-en-1-ol using the Appel reaction, following a literature method [21] (Scheme 1).

The preparation of the (*E*)-stereoisomer of substituted lactam **2** was as previously described [8], through *N*-alkylation in DMF with tributyl-(3-chloropropenyl)stannane in the presence of lithium bis(trimethylsilyl)amide (LHMDS) as a base. In our case, we used a bromine-substituted analog as the alkylation reagent (Scheme 1). Reaction and isolation of the product were unproblematic, with 68% yield, compared

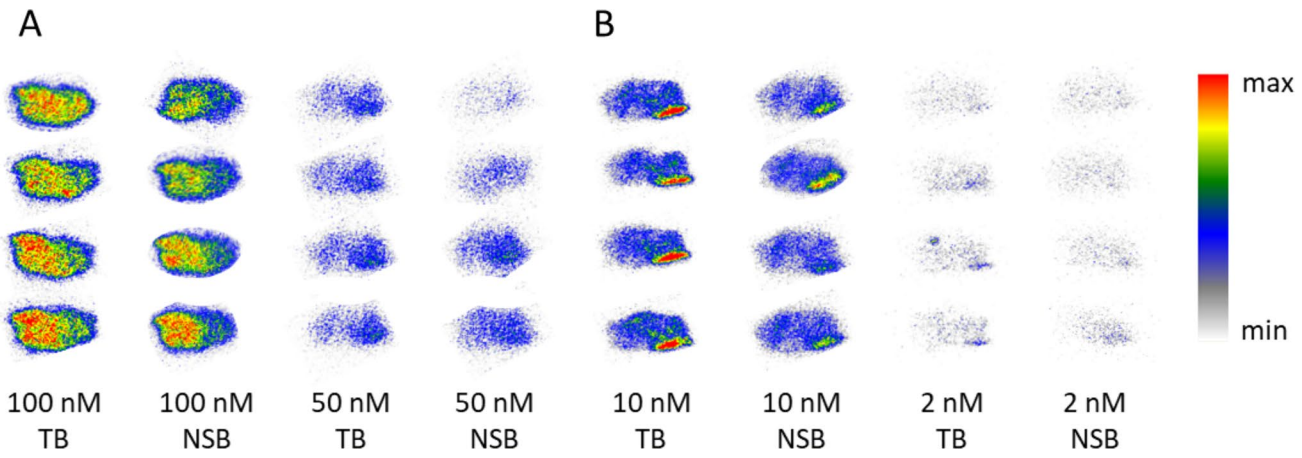

Fig. 3 *In vitro* autoradiography of [^{125}I]VPGIS191 in sagittal mouse brain cryostat Sect. (20 µm-thick). Non-specific binding was determined in the presence of excess of unlabeled GSK1482160 (10 µM). Exposure time 1 min (A) and 6 min (B). TB – total binding, NSB – nonspecific binding

to 88% as reported for the (*E*)-stereoisomer [8]. We suppose that our replacement of chlorine for bromine accounts for the lower yield.

We carried out the syntheses of the non-radioactive chromatographic VPGIS191 standard by two different methods, using either 82.2 µmol (Method I) or 10 nmol of precursor (Method II) (Scheme 1). Method I followed the procedure of Jin et al. [8], but replacing $CHCl_3$-MeOH (20:1–10:1, *v*/*v*) for hexane-EtOAc (4:1, *v*/*v*) as solvent in the silica-gel column purification. We obtained the product in 54% yield, as compared to the 90% reported by Jin et al. [8]. In the slightly modified Method II, we stopped the reaction with sodium ascorbate instead of sodium thiosulfate, with reaction time of 5 min instead of 15 min. We developed a new procedure for the SPE purification of the radiotracer, using 10% ethanol in water for SPE washing and 60% ethanol to elute the product, and had optimized the SPE purification for Bond Elute Plexa and alternately for Strata Phenomenex cartridges. Despite these measures, the product contained up to 0.01% tin-containing precursor according to HPLC-UV (Suppl. Mat. **Fig. S1**). We estimate a 100-fold margin of safety for the maximum possible carryover of tin from the synthesis, were this method eventually applied for human SPECT studies. We also tested the Sep pack C_{18} cartridge for SPE purification, which proved to retain the product even in 95% ethanol. Therefore, we used the optimized SPE procedure above for the radiosyntheses with ^{125}I and ^{123}I.

In vitro autoradiography of [^{125}I]VPGIS191 in mouse brain tissue

We performed in vitro autoradiography of **[^{125}I]VPGIS191** in mouse brain sagittal cryostat sections (Fig. 3), following an established procedure with optimized washing conditions by Kuhar et al. [22] as modified in [8]. The specific binding was invariably less than 50% of total binding, which disfavored quantitation by Scatchard analysis. Nonetheless, we were able in one trial to obtain estimates of K_d = 36 nM and B_{max} = 402 pmol/g, which closely matched corresponding affinity for **[^{123}I]TZ6019** in HEK cells (K_d = 19 nM) [8]. In what seems to be the first quantitation of $P2X_7$ sites in rodent brain cryostat sections, we find a rather high B_{max}, comparable to that seen for [^{3}H]PK11195 binding at microglial TSPO sites [23]. Despite this high B_{max}, the low affinity and high non-specific binding of **[^{125}I]VPGIS191** disfavored its use in quantitative autoradiography, and may likewise predict low signal-to-background in SPECT studies with this ligand (Fig. 4).

Conclusions

Several structural classes of radioligands for the $P2X_7$ receptor intended for PET or SPECT imaging have affinities in the range 1–20 nM (Table 1); among these, only the pyroglutamic acid derivative [^{123}I]TZ6019 is intended for SPECT imaging had 20 nM affinity in HEK cells [8], which may not suffice for visualization on $P2X_7$ sites in living brain. As an alternative to [^{123}I]TZ6019, we prepared its geometric isomer VPGIS191 as reference standard, and also labelled with iodine-123 for SPECT, or iodine-125 for autoradiography in vitro. Unlike the literature synthesis for TZ6019, our synthesis of **VPGIS191** employs a commercially available intermediate, namely (*Z*)-3-(tributylstannyl)prop-2-en-1-ol. We obtained the precursor in 68% yield, the reference standard VPGIS191 **VPGIS191** in 52% yield, ^{123}I labelled radiotracer in 71 ± 13% radiochemical yield, and ^{125}I labelled radiotracer in 85 ± 6% radiochemical yield. Despite its high

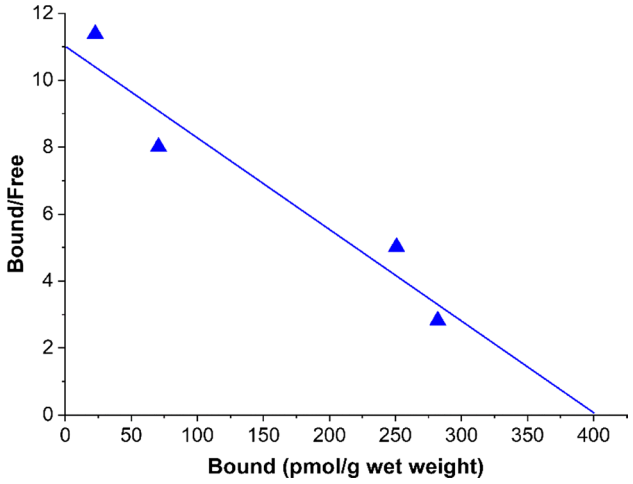

Fig. 4 Scatchard analysis of the saturable binding of [^{125}I]VPGIS191 in mouse brain sagittal cryostat sections. Each point indicates the mean of four determinations at 2, 10, 50, and 100 nM [^{125}I] VPGIS191.

non-specific binding in vitro, we obtained adequate estimates of the saturation binding parameters K_d (36 nM) and B_{max} (402 pmol/g) in mouse brain sections. The two-fold lower affinity of [^{125}I]VPGIS191 compared to the literature value for its geometric isomer TZ6019 seems in agreement with previously published comparisons of *Z*- and *E*-3-iodoallylated PET and SPECT tracers [17–20].

Supplementary Information The online version contains supplementary material available at https://doi.org/10.1007/s10967-023-09081-2.

Acknowledgements The authors appreciate valuable discussions with nuclear chemist prof. Ing. Jan John, CSc.; toxicologist prof. RNDr. Jiří Patočka, DrSc., PD Francisco Rafael López Picón, Ph.D.; Mag. Iris Maria Aichhorn, and nuclear chemist prof. Emma Hilda Kristina Aneheim, Ph.D. during the course of this research.

Author contributions Conceptualization: R.P., M.J., A.P. Synthesis and characterization of the compounds: A.M., M.J., T.Z. Experiments on animal samples: A.M., M.P., P.D. Supervision: M.J., P.B.D., S.L., P.C., R.P. and A.P. Original draft preparation: A.M., M.J., P.C., and A.P. Revision of the paper: A.M., M.J., P.C., M.P. and A.P.

Funding Open access publishing supported by the National Technical Library in Prague. This research was supported by a grant from the UCT Prague: A2_FPBT_2022_067 and the Ministry of Education, Youth and Sports of the Czech Republic (project EATRIS-CZ LM2023053, project CZ-OPENSCREEN LM2023052) and by project no. LX22NPO5107 (MEYS): Financed by EU – Next Generation EU.

Declarations

Animal experimentation approval Animal experiments were conducted in accordance with regulations and guidelines of the Czech Animal Protection Act (No. 246/1992), and with the approval of the Czech Ministry of Education, Youth, and Sports (MSMT-41830/2018-7) and the institutional Animal Welfare Committee of the Faculty of Medicine and Dentistry of Palacky University in Olomouc.

Conflict of interest The authors declare that they have no known competing financial interests or personal relationships that could have appeared to influence the work reported in this paper.

Supplementary Information Additional supporting information may be found online in the Supplementary material.

References

1. Leeson HC, Chan-Ling T, Lovelace MD, Brownlie JC, Gu B, Weible MW (2019) P2X$_7$ receptor signaling during adult hippocampal neurogenesis. Neural Regen Res 14:1684–1694. https://doi.org/10.4103/1673-5374.257510
2. Surprenant A, Rassendren F, Kawashima E, North RA, Buell G (1996) The cytolytic P2Z receptor for extracellular ATP identified as a P2x receptor (P2X$_7$). Sci (Washington D C) 272:735. https://doi.org/10.1126/science.272.5262.735
3. Takenouchi T, Sekiyama K, Sekigawa A, Fujita M, Waragai M, Sugama S, Iwamaru Y, Kitani H, Hashimoto M (2010) P2X$_7$ receptor signaling pathway as a therapeutic target for neurodegenerative diseases. Arch Immunol Ther Exp 58:91–96. https://doi.org/10.1007/s00005-010-0069-y
4. Chen Z, He L, Li LF, Chen LX (2018) The P2X$_7$ purinergic receptor: An emerging therapeutic target in cardiovascular diseases. Clin Chim Acta 479:196–207. https://doi.org/10.1016/j.cca.2018.01.032
5. Adinolfi E, Raffaghello L, Giuliani AL, Cavazzini L, Capece M, Chiozzi P, Bianchi G, Kroemer G, Pistoia V, Di Virgilio F (2012) Expression of P2X$_7$ receptor increases *in vivo* tumor growth. Cancer Res 72:2957–2969. https://doi.org/10.1158/0008-5472.can-11-1947
6. Zheng Q-H (2020) Radioligands targeting purinergic P2X$_7$ receptor. Bioorg Med Chem Lett 30:127169. https://doi.org/10.1016/j.bmcl.2020.127169
7. Gao MZ, Wang M, Green MA, Hutchins GD, Zheng QH (2015) Synthesis of C-11 GSK1482160 as a new PET agent for targeting P2X(7) receptor. Bioorg Med Chem Lett 25:1965–1970. https://doi.org/10.1016/j.bmcl.2015.03.021
8. Jin H, Han JB, Resing D, Liu H, Yue XY, Miller RL, Schoch KM, Miller TM, Perlmutter JS, Egan TM, Tu ZD (2018) Synthesis and in vitro characterization of a P2X$_7$ radioligand I-123 TZ6019 and its response to neuroinflammation in a mouse model of Alzheimer disease. Eur J Pharmacol 820:8–17. https://doi.org/10.1016/j.ejphar.2017.12.006
9. Gao M, Wang M, Meyer JA, Territo PR, Hutchins GD, Zarrinmayeh H, Zheng Q-H (2019) Synthesis and *in vitro* biological evaluation of new P2X7R radioligands [^{11} C]halo-GSK1482160 analogs. Bioorg Med Chem Lett 29:1476–1480. https://doi.org/10.1016/j.bmcl.2019.04.018

10. Lord B, Ameriks MK, Wang Q, Fourgeaud L, Vliegen M, Verluyten W, Haspeslagh P, Carruthers NI, Lovenberg TW, Bonaventure P, Letavic MA, Bhattacharya A (2015) A novel radioligand for the ATP-gated ion channel P2X7: [^{3}H]JNJ-54232334. Eur J Pharmacol 765:551–559. https://doi.org/10.1016/j.ejphar.2015.09.026
11. Janssen B, Vugts DJ, Wilkinson SM, Ory D, Chalon S, Hoozemans JJM, Schuit RC, Beaino W, Kooijman EJM, van den Hoek J, Chishty M, Domene A, Van der Perren A, Villa A, Maggi A, Molenaar GT, Funke U, Shevchenko RV, Baekelandt V, Bormans G, Lammertsma AA, Kassiou M, Windhorst AD (2018) Identification of the allosteric $P2X_7$ receptor antagonist [^{11} C]SMW139 as a PET tracer of microglial activation. Sci Rep 8:1–10. https://doi.org/10.1038/s41598-018-24814-0
12. Huang G, Lu X, Qiu Y, Bi L, Ye P, Yang M, Shen Y, Jin H, Han J (2022) Hetero-aryl bromide precursor fluorine-18 radiosynthesis and preclinical evaluation of a novel positron emission tomography (PET) tracer [^{18}F]GSK1482160. Bioorg Med Chem 73:116996. https://doi.org/10.1016/j.bmc.2022.116996
13. Gao M, Wang M, Glick-Wilson BE, Meyer JA, Peters JS, Territo PR, Green MA, Hutchins GD, Zarrinmayeh H, Zheng Q-H (2018) Synthesis and preliminary biological evaluation of a novel P2X7R radioligand [^{18}F]IUR-1601. Bioorg Med Chem Lett 28:1603–1609. https://doi.org/10.1016/j.bmcl.2018.03.044
14. Gao M, Wang M, Glick-Wilson BE, Meyer JA, Peters JS, Territo PR, Green MA, Hutchins GD, Zarrinmayeh H, Zheng Q-H (2019) Synthesis and initial in vitro characterization of a new P2X7R radioligand [^{18}F]IUR-1602. Appl Radiat Isot 144:10–18. https://doi.org/10.1016/j.apradiso.2018.11.006
15. Territo PR, Meyer JA, Peters JS, Riley AA, McCarthy BP, Gao M, Wang M, Green MA, Zheng Q-H, Hutchins GD (2017) Characterization of ^{11} C-GSK1482160 for targeting the $P2X_7$ receptor as a biomarker for neuroinflammation. J Nucl Med 58:458. https://doi.org/10.2967/jnumed.116.181354
16. Han J, Liu H, Liu C, Jin H, Perlmutter JS, Egan TM, Tu Z (2017) Pharmacologic characterizations of a P2X7 receptor-specific radioligand, [^{11} C]GSK1482160 for neuroinflammatory response. Nucl Med Commun 38:372–382. https://doi.org/10.1097/mnm.0000000000000660
17. Elmaleh DR, Fischman AJ, Shoup TM, Byon C, Hanson RN, Liang AY, Meltzer PC, Madras BK (1996) Preparation and biological evaluation of iodine-125-IACFT: a selective SPECT agent for imaging dopamine transporter sites. J Nucl Med 37:1197–1202
18. Xu R, Lord SA, Peterson RM, Fergason-Cantrell EA, Lever JR, Lever SZ (2015) Ether modifications to 1-[2-(3,4-dimethoxyphenyl)ethyl]-4-(3-phenylpropyl)piperazine (SA4503): Effects on binding affinity and selectivity for sigma receptors and monoamine transporters. Bioorg Med Chem 23:222–230. https://doi.org/10.1016/j.bmc.2014.11.007
19. Lever SZ, Xu R, Fan K-H, Fergason-Cantrell EA, Carmack TL, Watkinson LD, Lever JR (2012) Synthesis, radioiodination and in vitro and in vivo sigma receptor studies of *N*-1-allyl-*N*´-4-phenethylpiperazine analogs. Nucl Med Biol 39:401–414. https://doi.org/10.1016/j.nucmedbio.2011.10.001
20. Lever JR, Scheffel UA, Stathis M, Musachio JL, Wagner HN Jr (1990) In vitro and in vivo binding of (*E*)- and (*Z*)-*N*-(iodoallyl) spiperone to dopamine D_2 and serotonin 5-HT2 neuroreceptors. Life Sci 46:1967–1976. https://doi.org/10.1016/0024-3205(90)90513-q
21. Thompson AM, Sutherland HS, Palmer BD, Kmentova I, Blaser A, Franzblau SG, Wan BJ, Wang YH, Ma ZK, Denny WA (2011) Synthesis and structure-activity relationships of varied ether linker analogues of the antitubercular drug (6*S*)-2-nitro-6-{[4-(trifluoromethoxy)benzyl]oxy}-6,7-dihydro-5*H*-imidazo[2,1-b][1,3]oxazine (PA-824). J Med Chem 54:6563–6585. https://doi.org/10.1021/jm200377r
22. Kuhar MJ (2001) In vitro autoradiography. Curr Protoc Pharmacol Chap 8. https://doi.org/10.1002/0471141755.ph0801s00.
23. Pedersen MD, Minuzzi L, Wirenfeldt M, Meldgaard M, Slidsborg C, Cumming P, Finsen B (2006) Up-regulation of PK11195 binding in areas of axonal degeneration coincides with early microglial activation in mouse brain. Eur J Neurosci. https://doi.org/10.1111/j.1460-9568.2006.04975.x